**HIGHLIGHTS**

- Soil macroaggregates (4-1 and 1-0.25 mm) thin sections have been investigated
- Optical microscopy and SEM-EDS allowed the *in situ* analysis of OM in macroggregates
- Both physical occlusion and mineral interactions stabilized OM in macroaggregates
- The highest OM stabilization by both mechanisms was in fine macroaggregates
- In fine macroaggregate, both OM accumulation and functionality maintenance occurred

**Title**

# New insights into organic carbon stabilization in soil macroaggregates: an *in situ* study by optical microscopy and SEM-EDS technique

Authors

Guidi Patrizia (1), Falsone Gloria (1), Wilson Clare (2), Cavani Luciano (1), Ciavatta Claudio (1), Marzadori Claudio (1)

Author Affiliations

(1) Dipartimento di Scienze e Tecnologie Agro-alimentari, Alma Mater Studiorum Università di Bologna, 40127 Bologna (I)

(2) Biological and Environmental Science, University of Stirling, FK9 4LA Stirling (UK)

Corresponding author

Gloria Falsone, email gloria.falsone@unibo.it

**ABSTRACT**

The purpose of this study was to investigate the *in situ* characterization of organic matter (OM) within soil macroaggregates, and to assess the relationships between OM characteristics and macroaggregate size indicating different OM stabilization mechanisms. Optical micro-morphological investigations, coupled to SEM-EDS (scanning electron microscopy and energy X-ray spectroscopy) technique, were carried out on thin sections of 1-4 and 0.25-1 mm soil aggregates (coarse and fine macroaggregates, respectively) from 0-20 cm soil layer corresponding to A horizon of four different sites in which soil structure were not disturbed by tillage.

The intraggregate porosity, measured by image analysis of four different size classes (<50, 50–100, 100–200, >200 μm), showed that fine macroaggregates were significantly less porous (3.70-6.71% of total porosity) and had higher presence of the finest pore class (<50 μm) compared to coarse macroaggregates (5.93-9.08% of total porosity), independently from sites. The percentage of organic matter forms (OMFs) identified by optical investigation was significant higher in fine (13.5-17.7%) than in coarse (4.19-8.27%) macroaggregates. In particular, fine macroaggregates were richer in red and black amorphous organic forms, which were characterized by the highest values of Al:C, Fe:C and Ca:C molar ratios. These findings suggested thus an accumulation of OM in fine macroaggregates than in coarse macroaggregates occurred. It was probably due to a more efficient OM stabilization in fine than in coarse macroggregates related to both physical occlusion (lower porosity and smaller pore size) and organo-minerals interaction (higher presence of OMFs characterized by the highest Al:C, Fe:C and Ca:C ratios),

The OM exposure index (EI), a measurement of the OM surface exposed to pores and thus potentially available for microbial activity, was unexpectedly higher in fine than in coarse macroaggregates (EI: 0.48-0.79 and 0.25-0.58 $mm^{-1}$ in fine and coarse macroaggregates, respectively). However, the accessibility of OM defined by the EI seemed to facilitate neither the oxidative transformation nor the damage of enzyme activities, being the EI positively related to C:N ratio (r=0.66), negatively to $\delta^{13}C$ values (r=-0.74) and positive to the geometric mean of the five assayed enzyme activities related to C-cycle (r=0.79). Therefore, even more potentially exposed, in fine macroaggregates the OM was not accessible to microorganisms due to the

43 effective physical occlusion, and thus both accumulation of few transformed OM and maintenance of
44 functionality related to C-cycle occurred.
45 The OM stabilization in macroaggregates thus involved both physical occlusion and organo-metals/mineral
46 phase interactions processes. Both these processes are often related to microaggregates rather than
47 macroaggregates. Our findings thus seem to provide a new insight for studying the potentiality of OM
48 stabilization and C sequestration in soil macroaggregates.
49

**KEYWORDS**

Macroaggregate size; aggregate thin sections; optical microscopy; SEM-EDS; physical occlusion; organo-mineral interactions.

## 1. INTRODUCTION

The largest amount of organic C in terrestrial ecosystems is in the soil and it is three time the amount of C in the atmosphere and four time that in the biota (Janzen, 2004). The persistence of this high amount of organic matter (OM) in soil depends on many factors including land use, edaphic factors and climate (Smith et al., 2008), and can be altered by human activities, which can indeed have contrasting effects (Bai et al., 2018; Baude et al., 2019; Lal, 2004a; Lal, 2004b; Lal et al., 2015). One of the objectives of the current soil science research is to model, in a reliable way, the flow of C from, within, and to the soil in order to allow the assessment of the different soil properties and management practices applied. To date, one of the main difficulties in reaching this goal is given by the lack of sufficiently detailed knowledge on the processes that govern the persistence of the soil OM (Schmidt et al., 2011).

Several authors consider that, for a mechanistic understanding and modelling of soil OM decomposition and stabilization, it is crucial to improve knowledge on processes such as occlusion of organic matter within aggregates and sorption of organics onto mineral surfaces (Kögel-Knabner et al., 2008). Conant et al. (2011) proposed a conceptual model defining the resistance of soil OM to decomposition as being due to its chemical structure and its physicochemical protection. The former referred to the de-polymerization process, the latter to adsorption/desorption on mineral surface and aggregate turnover. Recently, Wiesmeier et al. (2019) stressed the role of physical protection within aggregates for soil OM persistence, stating that physical protection, and therefore the aggregation process itself, must be considered as an important mechanism for stabilization of organic C.

The physical protective capacity of aggregates to soil OM is related to the spatial separation of substrate and microorganisms, as well as to reduced microbial activity due to a lower diffusion of gasses into and within aggregates (Mikutta et al., 2006; Six et al., 2002). Kravchenko et al. (2015), combining $CO_2$ respiration measurements with X-ray computed micro-tomography imaging, demonstrated a feed-forward relationship between particulate organic matter decomposition and pore connections in intact soil samples. Furthermore, organo-mineral associations acting in soil OM protection can be considered as structural units of soil

aggregates and nanoparticulate fractions of the smaller aggregates themselves (Totsche et al., 2017), and are, therefore, strictly related to the aggregate formation process.

Six et al. (2000) postulated that SOM stabilization is based on microaggregate (<0.25 mm) formation within macroaggregates (>0.25 mm), with C in microaggregates stabilized and sequestered for the long-term. Macroaggregates would instead provide minimal C physical occlusion (Six et al., 2004). The efficiency of macro- and microaggregates in soil OM stabilization is due to the different mechanisms that generate aggregates of different size, as extensively described (e.g., Six et al., 2004). However, the role of macroaggregates is essential in soil OM stabilization; macroaggregates being important environment where both organic C is preferentially accumulated and microaggregate formation occurs (Gioacchini et al., 2016; Six et al., 2000).

In addition to the aggregate size, the extent of the C transformation and stabilization in aggregates can be influenced by the network of the intraggregate pores (Toosi et al., 2017), and by the OM exposure to the pore surface (Ananyeva et al., 2013). The exposure of the OM to the pores surface can influence the contact with the gaseous and biotic phase of the soil, two fundamental factors in the transformation OM processes. We suggest thus that the localization of the OM within the aggregates is an aspect that needs to be taken into account and demands in-depth investigation.

Optical micro-morphological investigations of soil aggregate thin sections allows researchers to localize soil OM in an undisturbed physical space within aggregates and, coupling them with SEM-EDS analysis, to investigate *in situ* characteristics of OM. Considering that C preferentially accumulates in macroaggregates, and that the processes leading to the long-term soil OM stabilization begins within macroaggregates (i.e., the microaggregates formation begins within macroaggregates), we believe that a study of OM properties within macroaggregates can provide new insights into the understanding of the processes of organic carbon preservation into soil aggregates.

For this, optical micro-morphological investigations, coupled SEM-EDS technique, of thin sections of macroaggregates of different size (1-4 mm coarse macroaggregates, 0.25-1 mm fine macroaggregates) were carried out to study *in situ* OM properties. In order to increase our knowledge on soil OM persistence, the

current research examined these microfeatures in soils characterized by different site conditions in two mountain and plain areas in the Northern Italy.

Specifically, this study focused on (i) the *in situ* characterization of soil organic matter within coarse and fine macroaggregates from soil in different site conditions, and (ii) the existence of relation between OM characteristics and macroaggregate size suggesting specific OM stabilization processes. We investigated four soils from sites that differed in key drivers of OM persistence, such as climate, soil properties and management (Wiesmeier et al., 2019) because we would test if the hypothesized relationships between OM characteristics and macroaggregate size were similar among different sites (i.e., sites which differed in climate, soil properties and management) and thus if a certain size-effect exists transgressing the environmental key properties.

## 2. MATERIALS AND METHODS

### *2.1. The study area*

In this study we investigated both mountain and plain areas of different altitudes in the Emilia Romagna region (Northern Italy). The mountain area was located at Monzuno in the Appennine mountain, while the plain area was at Cadriano in the Po Valley (Table 1). The soils in the mountain area formed on limestone-marl and pelitic-sandstone stratifications, while those in the plain area develop on conoids, i.e. sedimentary bodies consisting of a clastic sediment accumulation. Both soils are ascribed to Inceptisols (Soil Survey Staff, 2014) as evinced from the Regional Soil Survey Service database (Regione Emilia Romagna, 2018). The climate of the mountain area is characterized by mean annual temperature of 11.6°C and mean annual precipitation of 967 mm, while in plain area by 12.9°C and 645 mm, respectively.

In both areas we selected two sites on the basis of soil management (Table 1), avoiding agricultural sites subject to annual tillage operations that would strongly affect soil aggregation (Bronick and Lal, 2005). In the mountain area, we thus selected a 16-yrs old oak wood (M-OW) and a 5-yrs old alfalfa (M-AA.). In the plain area we investigated an experimental walnut grove of the cv. Lara in place since 2001 selecting one fertilized area (P-FF) receiving 90 kg urea $ha^{-1}$ $y^{-1}$ as granular urea and one non-fertilized control area without urea

distribution (P-NF). In each site, two different plots have been selected and pits wide about 0.3 m were dug. From each pit, the 0-20 cm soil layer corresponding to A horizon was collected. The main physico-chemical properties of the fine earth of 0-20 cm topsoil were reported in Table 1S.

All soil samples were air dried at room temperature and sieved in order to obtain the macroaggregate fraction (>0.25 mm; Six et al. 2000; Tisdall and Oades, 1982). The macroaggregates have been further divided by dry-sieving into coarse macroaggregates (1-4 mm) and fine macroaggregates (0.25-1 mm) using a 1 mm sieve in agreement with experimental evidence (e.g., Legout et al., 2005; Lu et al., 2016) indicating that aggregates >1 mm might have lower stability, and thus higher turnover, than aggregates <1 mm.

*2.2. Soil aggregate thin sections preparation*

The aggregates in both macroaggregate classes have been gently mixed and at least 25 and 50 aggregates have been randomly kept for the preparation of thin section of the coarse and fine macroaggregate, respectively. Water was removed from the aggregates by air-drying to avoid C losses during the acetone replacement drying process. No accommodating crack voids were identified in the air-dried thin sections, suggesting that shrinkage and cracking during the drying process had been minimal. The method for preparing thin section was based on Takeda (1988) and Tippkötter et al. (1986). Blocks of aggregates were obtained by impregnation of aggregates samples with polyester resin. The blocks have been then cut along a diameter plane, shaven out and glued to the slide. The slices were thinned to a standard thickness of 30-40 µm, using the Logitech precision lapping machine. The slices were further reduced to few µm and hand-polished by rubbing the slices on paper coated using the birefringence colours of the minerals as indicated in the Michel-Levy paper which reports the birefringence colours of individual minerals according to their thickness. Finally, aggregates thin sections (28 x 48 mm) were polished using diamond paste. The slides were not cover-slipped since the organic microfeatures in these thin-sections were to be analysed for their elemental composition by scanning electron microscope (SEM) equipped with an EDS probe.

156 *2.3. Optical micromorphology observations, image analysis of pores and organic components in the*
157 *aggregate thin sections*
158 Conventional descriptions of thin sections were made at 40X following the guidelines of Stoops (2003) and
159 Fitzpatrick (1980). To achieve our research aim, the area of interest in each thin section in this study
160 corresponded to the intraggregate area. Measurements on aggregates close to the edge of the thin sections
161 or having inside/near artificial bubbles were avoided, and consequently in coarse macroaggregate thin
162 sections from 9 to 16 single aggregates were analysed for each site, while in fine macroaggregate thin
163 sections from 23 to 41 aggregates were investigated. Optical observations have been carried out using a
164 polorised microscope Olimpus BX50.
165 For image analysis of intra-aggregates porosity and organic matter, high-resolution images were captured at
166 40x using a digital camera, and connected to a computer equipped with an images frame grabber. Captured
167 images were then available for computerised analysis carried out by AnalySIS v 510 (Olympus Soft Imaging
168 Solutions GmbH) image analysis software. Image analysis provides quantitative information from the
169 scanned image.
170
171 *2.3.1. Total porosity and pore size distribution*
172 To measure pores, multiple images of the same representative aggregates were taken under both plane (PPL;
173 Figure S1-a) and crossed polarized light (XPL) at 0.5 and 15° (Falsone et al., 2014). This was necessary to
174 distinguish between pores and quartz, since both were translucent under PPL. These images were additively
175 combined and the result inverted. The inverted images were multiplicatively layered with a natural light
176 image to produce a composite binary image in which minerals were readily distinguished from voids, with
177 minerals and soil matrix represented by black pixels and pores by white pixels (Figure S1-b; Hallaire et al.,
178 2000; Nakatsuka and Tamura, 2016). To exclude any electronic noise and difficulties in removing quartz, the
179 minimum size for detecting pores was set at 100 $\mu m^2$.
180 The pores were classified according to four different size classes (Pagliai et al,. 2004; Zhou et al., 2012): <50,
181 50–100, 100–200, >200 µm, on the basis of their equivalent diameters. The total surface of pores and the

surface of each pore classes were measured. The percentage of total porosity (total porosity %, i.e., total surface of pores/surface of investigated area) and pore size distribution (% of <50, 50–100, 100–200, >200 µm; i.e., surface of each pore class/total surface of pores) were thus calculated.

### *2.3.2. Total surface of organic matter forms (OMFs) and their distribution*

Under PPL and XPL conditions, the organic forms were identified and categorized as being either organ or amorphous in form (Babel, 1975; Figure S2). Once classified according to their form, organic components have been further described according to the extent of their decomposition following the classification proposed by Fitzpatrick (1993) where amorphous forms were strongly decomposed organic fragments, and were further described by their colour, with change in colour from yellow to red and black indicating greater decomposition due to oxidative and microbial processes (Bullock et al., 1985; Figure 2). A manual delimitation of each organic component has been provided using image analysis software within PPL images (Figure S1-c). Images were thus segmented selecting for organic fragments, and the total area of organic fragments and the area of each class of organic features was measured.

The percentage of total surface of organic forms (organic matter forms %, i.e., surface of organic forms/ surface of investigated area) was calculated. The distribution of different organic components recognised (% of organs and amorphous forms, classified according to their decomposition degree and colour, respectively) was also calculated (i.e., surface of each organic form/surface of investigated area).

### *2.3.3. Organic matter-pores contact: the exposure index (EI)*

The images obtained by organic components analysis was exported and stacked upon the binary pore image thereby forming a map showing the distribution of organic matter in relation to soil pores. It was thus possible to identify the surface of organic matter in contact to the pores and to measure the length of contact perimeter between the two features. Then, the total length of the contact perimeter (in mm) was normalized by the total area of organic form (in $mm^2$), in order to obtain a measure of the proportion of the organic matter surface in contact to the pore. For each sample, an index, called exposure index (EI; $mm^{-1}$) was

208 calculated. The EI gives information about the organic matter-pores contact, and therefore on the potential
209 physical exposure of organic matter to the microbial activity (Young et al., 2008).
210
211 *2.4. SEM-EDS analysis on the aggregate thin sections*
212 Polished thin sections were analysed using an environmental scanning electron microscope (SEM) and
213 elemental data were collected by energy-dispersive spectroscopy (EDS) detector using ZEISS SEM systems
214 (EVO MA15) linked to an Oxford Instruments INCA X-max detector with an 80-$mm^2$ SDD. For this work, the
215 instrument setup was: low vacuum conditions (>30 kPa), accelerating voltage of 5-20 keV, process time of
216 5.0, working distance of 8.5 mm, spot-size between 500-560. EDS analysis was performed at high
217 magnifications (500-1000x). The microanalysis was carried out for the detected organic features (Figure S2)
218 in coarse and fine macroaggregates. About 50 points were scored for each organic feature. Data was
219 normalized to 100%, giving a semi-quantitative measure of elemental concentrations. Thus elemental molar
220 ratios are discussed in this work rather than absolute concentrations. Additionally, using elemental molar
221 ratios any C resin effect has been avoided. The ratios are thus being interpreted relative to one another rather
222 than being presented as actual soil ratios.
223 In this work we took into account the Al:C, Fe:C and Ca:C molar ratios as indicators of the degree of organic-
224 metals/minerals interactions (Falsone et al., 2014).
225
226 *2.5. Aggregate properties measured on aggregate fractions separated by sieving*
227 In order to check the relationships between the features measured *in situ* on aggregate thin sections and
228 chemical and biochemical aggregate properties, the organic carbon, total nitrogen, $\delta^{13}C$ signature and
229 enzyme activities related to carbon cycle have been measured on each macroaggregate class obtained by
230 dry-sieving.
231
232 *2.5.1. Organic C, total N and $\delta^{13}C$*

For each aggregate fraction separated by dry-sieving, a representative subsample has been kept and finely ground (<0.5 mm). The total organic C (g C $kg^{-1}_{aggregate}$) and total N (g N $kg^{-1}_{aggregate}$) concentration were determined on about 10-15 mg of finely ground aggregate subsamples by dry combustion (CHNS-O Elemental Analyser 1110, Thermo Scientific GmbH, Dreieich, DE). The relative abundance of C stable isotopes was determined by continuous flow- isotope ratio mass spectrometry (CF-IRMS) using an isotopic mass spectrometer Delta V advantage (Thermo- Finnigam, DE). The values were then expressed as $\delta^{13}C$, as deviation in parts per thousand compared to the universal reference standard.

*2.5.2. The geometric mean of enzyme activities (GMea)*

For each aggregate fraction separated by dry-sieving, enzyme activities have been measured using about 2 g of samples. The geometric mean of the assayed enzyme activities (GMea) was used as a comprehensive index of soil quality in order to compare enzyme activities in coarse and fine aggregates (Liu et al., 2013). For each aggregates class the geometric mean of the assayed enzyme activities (GMea) was calculated as:

$$GMea = \sqrt[5]{\beta - GLU \cdot \alpha - GLU \cdot N - AG \cdot \beta - XYL \cdot \beta - CEL} \quad (1)$$

where β-GLU, α-GLU, N-AG, β-XYL and β-CEL were β-glucosidase, α-glucosidase, N-acetyl β-glucosaminidase, β-xylosidase, β-cellobiosidase, respectively. These enzyme activities were chosen on their relevance for C cycle (Liu et al., 2013, Qin et al., 2010). The activity of these five extracellular hydrolytic enzymes was determined using MUF conjugates at final concentrations (Microplate fluorometer infinite200, TECAN, Männedorf, CH) ensuring substrate saturating conditions in according to Giacometti et al. (2014).

*2.6. Statistical analysis*

Differences in the micromorphological features (porosity, organic forms, EI) between coarse and fine macroaggregaes (size factor) were checked by the one-way ANOVA.

Differences in the molar ratio (Al:C, Fe:C and Ca:C), determined from EDS analysis, among organic forms and between coarse and fine macroaggregates in thin section were tested by the one-way ANOVA.

The assumption of ANOVA was tested by Shapiro-Wilks test for normality and data distribution and Levene test for homogeneity of variances.

The relationships between EI micromorphological property and both the chemical and biochemical properties measured on the aggregates were evaluated using the Pearson's correlation coefficient.

The threshold used for significance in all statistical tests was set at 0.05. All data treatments were carried out using R *agricolae* package (R core team, 2019).

## 3. RESULTS

### *3.1. Porosity*

The total detectable porosity, measured in the intraggregates space, ranged from 5.93 to 9.08% and from 3.70 to 6.71% in coarse and fine macroaggregates, respectively (Table 2). Porosity varied significantly based on size factor ($p<0.001$), and the fine macroaggregates were less porous than the coarse ones (Table 2). Within each aggregate class, among sites no differences in the intraggregate porosity were found.

Figure 1 (a-b) shows the pore size distribution (PSD) in the different aggregates. The PSD was significantly influenced by the size factor ($p <0.01$; Figure 1-c). The pores >200 μm were only present in coarse macroaggregates, while in fine macroaggregates pore <50 μm predominated. Fine macroaggregates, therefore, were significantly less porous and showing finer porosity compared to coarse macroaggregates. Between sites, no differences in the PSD were found (Figure 1-c).

### *3.2. Organic C concentration and organic matter forms (OMFs)*

The concentration of organic C in aggregates, measured on ground samples, varied from 6.6 and 49.6 g $kg^{-1}$ and from 7.8 and 52.4 g $kg^{-1}$ in coarse and fine macroaggregates, respectively (Table 2). The organic C content of fine and coarse macroaggregates was therefore characterized by a high variability, but it was possible to observe a tendency for which the accumulation of C significantly increased passing from the coarse to the fine macroaggregates within each site (p always <0.01; Table 2). The percentage of OMFs, measured on

aggregate thin sections, varied from 4.19 to 8.27 and from 13.54 to 17.75% in coarse and fine macroaggregates, respectively (Table 2), confirming that accumulation of organic matter was higher in fine than in coarse macroagrregates ($p<0.001$). The percentage of OMFs on macroaggregates thin section and organic C concentration measured by dry combustion on ground aggregates showed thus a significant similar trend ($r=0.567$, $p<0.05$).

*3.3. OMFs distribution and Al:C, Fe:C and Ca:C molar ratios*

The OMFs detected on thin sections were differently distributed between aggregates (Table 3): the organs have been detected only in coarse macroaggregates of mountain sites, while the organic amorphous forms have been found both in coarse and fine macro-aggregates. The lack of organs in the plain area evidenced difference according sites, which was confirmed also for amorphous forms ($p<0.05$). However, independently from the sites, according to the size factor the fine macroaggregates were clearly the richest in red and black organic amorphous forms ($p<0.001$).

Coupling the optical analysis to the SEM-EDS technique, it was possible to perform a semi-quantitative measurement of the element concentrations for each identified OMFs class. In particular, Al:C, Fe:C and Ca:C molar ratios of each OMFs class in coarse and fine macro-aggregates were determined (Figure 2). The morphologically recognised OMFs showed different values of molar ratios. In particular, red and black amorphous forms were characterized by the highest values of Al:C and Fe:C ($p<0.05$) and black amorphous forms had also the highest values of Ca:C molar ratios ($p<0.05$). This occurred both in coarse and fine macroaggregates.

*3.4. Exposure Index (EI)*

The EI values (Figure 3) varied from 0.25 to 0.58 $mm^{-1}$ in coarse macroaggregates and from 0.48 to 0.79 $mm^{-1}$ in fine macroaggregates, being significantly higher in fine macroaggregates ($p<0.05$). Figure 4 showed the relationships between EI values and both C/N ratio and $\delta^{13}C$ values. Specifically, EI values was positively

correlated to the C/N ratio and negatively to the $\delta^{13}C$ values. The EI was significantly positively correlated also to GM*ea* (Figure 5).

## 4. DISCUSSION

### *4.1 The effect of macroaggregate size on OM characteristics*

One of the objectives of our work was to characterize soil organic matter (OM) fractions according to their specific physical location within the fine and coarse macroaggregates (*in situ*). Technically this was performed through optical investigation of aggregate thin sections which allowed us the *in situ* identification and quantification of organic matter forms (OMFs). The quantification of OM was also performed on ground samples by the well-standardized dry combustion method, which provides the quantification of the whole organic C in disturbed samples without any distinction among different forms. The quantification of OM content in the aggregates obtained by the two methods (i.e., the content of OC in ground aggregates and the presence of OMFs detected on aggregate thin section) showed similar trend and the data was significantly related.

The *in situ* quantification of OMFs showed that fine macroaggregates were richer in organic matter than coarse ones. Organic C accumulation in small aggregates is often reported (Six et al., 2000; Six et al., 2004; Tisdall and Oades, 1982), and in general this C-enrichment refers to microaggregates (i.e, aggregate <0.25 mm). Our findings thus showed that C accumulation can occur also in small macroaggregates of 0.25-1 mm size class. Additionally, our data showed that OC accumulation in fine macroaggregates was coupled to a decrease in porosity. In fact, the effect of macroaggregate size was also observed in the aggregate porosity, with the lowest porosity and the smallest pore size in the fine macroaggregate class. In our opinion, thus, the lowest porosity and smallest pore size in fine macroaggregates could enhance the persistence of OM. The effect of pores network on soil OM stabilization has been in fact observed by several authors. Toosi et al. (2017) demonstrated by their long-term experiment that, in natural succession system, the abundance of specific size classes of pores affected OM decomposition and thus its chemistry in macroaggregates. Kravchenko and Guber (2017) reported experimental evidences indicating pores of 30-90 μm in size as drivers

in processes of organic carbon decomposition. Ananyeva et al. (2013) showed that abundance of 40-70 μm pores was negatively correlated with levels of organic carbon in macroaggregates, suggesting that aggregates with great amount of such pores poorly protected organic matter. Quigley et al. (2018) agreed that pores of 40–90 μm size range are associated with quick organic C decomposition, while pores <40 μm tend to be associated with C protection. Yang et al. (2019) suggest that total porosity has a significant role, increasing soil aggregate organic carbon respiration. With regard to our data, we suggest that the highest total porosity could have favored a greater degradation of organic matter in coarse macroaggregates, and that conversely the greatest percentage of pores <50 μm in fine macroaggregates, according to cited authors, could have contributed to organic matter storage within them. Therefore, in our study the physical occlusion would be more efficient in fine macroaggregates than in coarse ones.

The effect of size classes of macroaggregates on physical occlusion seemed to transgress that of the site conditions, being both porosity and OMFs amount similar within fine and coarse macroaggregates. This finding was quite unexpected, because site conditions (climate, parent material, soil texture, soil OM, etc.) are considered as key factors in the aggregation process (e.g., Bronick and Lal, 2005; Saker et al., 2018). However, in our study a certain site effect has been detected on organic C content of ground aggregates. Thus, even if clearly the aggregate size strongly affected the physical occlusion of OM, we can not completely excluded a specific site effect on OM stabilization. The OMFs distribution in fact differed among sites: in the aggregates from the soils located in the plain areas organs completely lacked while they were present in the coarse macroaggregates of soils in the mountain areas. Fitzpatrick (1993) and Ismail-Meyer et al. (2018) suggested that organs consist of plant residues containing cells and represent thus less transformed soil OM. The presence of less transformed soil OM in mountain areas was indeed in agreement with the well-known slowing down of organic matter oxidative kinetics due to low temperature (e.g., Cardelli et al., 2019; De Feudis et al., 2019) allowing at higher altitude greater accumulation of less transformed OM in mountain soils than in plain ones. No general trend has been instead detected in amorphous forms, that according to Fitzpatrick (1993) and Falsone at al. (2014) are the end-product of organic residues transformation.

359 Independently from sites, other processes than physical occlusion might however contribute to the higher
360 accumulation of organic matter in fine than in coarse macroaggregates. Processes related to interaction of
361 OM with minerals/metals can in fact contribute to OM stabilization (Conant et al., 2011).
362 Our data showed that OM accumulation in fine macroaggregates was due to the organic amorphous forms,
363 being organs missing in fine macroaggregates. Additionally, SEM-EDS microanalysis showed that that red and
364 black amorphous forms had the highest Al:C, Fe:C and Ca:C molar ratios. These molar ratios are chemical
365 indicators of OM stabilization reflecting the interaction of OMFs with the soil mineral phase, and high molar
366 ratio values indicate stronger organo-mineral interactions (Brown et al., 2000). OM stabilization by mineral
367 interactions was thus mainly attributable to red and black OMFs. This was in agreement with the fact that
368 red and black amorphous organic forms are the end-product of organic residues transformation (Fitzpatrick,
369 1993), and that plant residues or particulate organic matter during decomposition become encrusted with
370 mineral particles and microbial by-products in macroaggregates (Six et al., 2004). It is well-known that these
371 interactions form the core of smaller aggregates within the larger ones, increasing soil OM stabilization in
372 microaggregates (Six et al., 2004). Our data allowed to detect that OM stabilization by mineral interactions
373 was not exclusive only of microaggregates, but efficiently occurred in fine macroaggregates.
374 Finally, the increasing of OM in fine macroaggregates should be ascribe to a more efficient OM stabilization
375 by both physical occlusion and organo-mineral interactions than in coarse macroaggregates.
376
377 *4.2 The dynamics of macroaggregates and organic matter stabilization*
378 The stabilization of organic matter in soil aggregate limits the oxidative processes, which generally drive the
379 transformation of soil OM. They may be in turn influenced by the degree of exposure of the OM to pores
380 interfacing with the gaseous and biotic phase (Geisseler et al., 2011). For this reason, an exposure index (EI)
381 of OM was calculated from the aggregate thin sections, and the relationships between EI and both C/N and
382 $\delta^{13}C$ values have been investigated. We interpreted the EI as an index of the potential physical exposure of
383 organic matter to microbial activity (Young et al., 2008), while the C/N ratio and the $\delta^{13}C$ signature provide
384 information the degree of transformation of organic matter. The C/N ratio is in fact an indicator of the whole

385 organic matter pool turnover (Bronick and Lal, 2005), and a high value of C/N suggests the presence of OM
386 with low transformed status. Isotopic carbon fractionation instead occurs during the process of organic
387 decomposition, leading to enrichment in $^{13}C$ due to oxidation of $^{12}C$ by microorganisms (Feng, 2002).
388 Consequently, lower values of $\delta^{13}C$ (more negative) correspond to less oxidized organic matter (Angers et al.,
389 1997). In our study, the C/N ratio and the $\delta^{13}C$ signature of fine and coarse macroaggregates were
390 significantly correlated ($r=-0.675$, $p<0.01$; Figure S3), confirming the data convergence related to the degree
391 of OM transformation.

392 Our findings showed that high values of EI was associated to fine macroggregates. This was quite unexpected,
393 because our data suggested higher physical occlusion of OM in fine macroaggregates due to lower porosity
394 and smaller pore size than in coarse macroaggregate. Because of the methodological procedure used for EI
395 determination, the EI measures the proximity of OM to the pore surface and thus assesses if the OM is
396 encapsulated in the soil matrix or exposed. The apparent discrepancy between great degree of OM exposure
397 and high physical occlusion in fine macroaggregates, in our opinion should be explain through the origin of
398 fine macroaggregate themselves. Organic residues must initially be accessible (i.e., exposed) to
399 microorganisms in order to form fine macroaggregates in coarse ones, in agreement with Six et al. (2004)
400 who described how the transformations of the OM represent the driving processes for the formation of fine
401 aggregates into coarse ones. Our hypothesis was thus that at least a part of the OM in fine macroaggregates
402 inherited its localisation from its initial accessibility in coarse macroaggregates, and that *i)* its initial
403 degradation allows the formation of fine macroaggregates causing OM encapsulation and *ii)* consequently
404 favouring OM stabilization. This seemed to be supported by positive correlation between EI and C/N ratio,
405 and the negative ones between EI and $\delta^{13}C$. They in fact indicated that high values of EI, typically associated
406 with fine macroaggregates, was related to OM form with lower degree of transformation. Additionally, EI
407 was positively linked to GMea. Thus, the apparent accessibility of OM defined by the EI did not compromise
408 the C-cycle functionally related to enzyme activities related to C-cycle and thus the soil functionality was
409 preserved (Wang et al., 2015; Wang et al., 2017).

410

## 5. CONCLUSIONS

This study offers a picture of the processes that are active within macroaggregates (1-4 and 0.25-1 mm) and which influence the transformation and stabilization of the OM as a function of its physical location. Our *in situ* investigation has allowed us to detect that:

- Coarse macroaggregates (1-4 mm) tended to be more porous and contained lower percentages of OMFs and organic C than and fine macroaggregates (0.25-1 mm).
- Fine macroaggregates accumulated OMFs characterized by a greater interaction with the mineral soil fraction, greater degree of exposure to the pores surface, lower degree of chemical transformation and higher maintenance of C-cycle functionality than in coarse macroaggregates.
- The fractions of the OM that have undergone the greatest chemical transformations (evaluated by C/N value and $\delta^{13}C$ signature) were in coarse macroaggregates and were not those that were more stable within the aggregates of the soil, in agreement with Schmidt et al. (2011).

The data of porosity, distribution of pores and organic forms determined by image analysis, confirmed that coarse and fine macroaggregates differed, and they were physically differentiated microhabitats for microorganisms. Specifically, fine macroaggregates had organic matter closer to the pores surface than in coarse macroaggregates probably due to the origin of fine macroaggregates themselves, whose genesis begins because of the decomposition of accessible particulate organic residues within coarse macroaggregates (Figure 6). In fine macroaggregates, the interaction between OM and metals and/or mineral phase and the physical occlusion of OM lead to its stabilisation (Figure 6).

Physical occlusion and interaction with minerals thus appeared as two complementary mechanisms enhancing OM stabilization in fine macroaggregates. Both these processes are often related to microaggregates (<0.25 mm) rather than macroaggregates (>0.25 mm) and further researches need on the study of their relative importance in fine macroaggregates. For example, the application of other techniques able to study intact (i.e, non-destroyed) aggregates and the three-dimensional nature of OM and pores distribution, might provide useful information on the physical protection of OM within soil

aggregates. However, our findings seem to provide a new insight for studying the potentiality of OM stabilization and C sequestration in soil macroaggregates.

**ACKNOWLEDGEMENTS**

This research did not receive any specific grant from funding agencies in the public, commercial, or not-for-profit sectors.

**REFERENCES**

Angers, D., Chenu, C., 1997. Dynamics of soil aggregation and C sequestration, in: Lal, R., Kimble, J.M., Follet, R.F., Stewart, B.A. (Eds.), Soil processes and the carbon cycle. Advances in Soil Sciences (col.), Boca Raton, CRC Press, pp. 199-223.

Ananyeva, K., Wang, W., Smucker, A.J.M., Rivers, M.L., Kravchenko A.N., 2013, Can intra-aggregate pore structures affect the aggregate's effectiveness in protecting carbon? Geoderma 287, 31-39.

Babel, U., 1975. Micromorphology of Soil Organic Matter, in: Gieseking, J.E. (Ed.), Soil Components. Springer, pp. 369-473.

Bai, Z., Caspari, T., Gonzales, M.R., Batjes, N.H., Mader, P., Bunemann, E.K., de Goede, R., Brussard, l., Xu, M., Ferreira, C.S.S., Reintam, E., Fan, H., Mihelic, R., Glavan, M., Toth, Z., 2018. Effects of agricultural management practices on soil quality: A review of long-term experiments for Europe and China. Agr. Ecosyst. Environ. 265, 1-7.

Baude, M., Meyer, B.C., Schindewolf, M., 2019. Land use change in an agricultural landscape causing degradation of soil based ecosystem services. Sci. Total Environ. 659, 1526-1536.

Bronick, C.J., Lal, R., 2005. Soil structure and management: a review. Geoderma 124: 3-22.

Brown, G.G., Barois, I., Lavelle, P., 2000. Regulation of soil organic matter dynamics and microbial activity in the drilosphere and the role of interactions with other edaphic functional domains. Eur. J. Soil Biol. 36, 177-198.

461 Bullock, P., Federoff, N., Jongerius, A., Stoops, G., Tursina, T., 1985. Handbook for soil thin section description.
462 Waine Research, Wolverhampton.
463 Cardelli, V., De Feudis, M., Fornasier, F., Massaccesi, L., Cocco, S., Agnelli, A., Weindorf, D.C., Corti, G. 2019.
464 Changes of topsoil under Fagus sylvatica along a small latitudinal-altitudinal gradient. Geoderma 344 164–
465 178.
466 Conant, R.T., Ryanu, M.G., Agren, G., Birge, H., Davidson, E.A., Eliasson, P.E., Evans, S.E., Frey, S.D., Giardina,
467 C.P., Hopkins, F.M., Hyvonen, R., Kirschbaum, M.U.F., Lavallee, J.M., Leifeld, J., Parton, W.J., Steinweg, J.M.,
468 Wallestein, M.D., Wettersted, J.A.M., Bradford, M. A., 2011. Temperature and soil organic matter
469 decomposition rates- synethesis of current knowledge and way forward. Global Change Biol. 17, 3392-3404.
470 De Feudis, M., Cardelli, V., Massaccesi, L., Trumbore, S.E., Vittori Antisari, L., Cocco, S., Corti, G., Agnelli, A.
471 2019. Small altitudinal change and rhizosphere affect the SOM light fractions but not the heavy fraction in
472 European beech forest soil. Catena 181, 104091.
473 Falsone, G., Wilson, C.A., Cloy, J.M. Graham, M.C., Bonifacio, E., 2014. Relating microfeatures of organic
474 matter to C stablisation: optical microscopy, SEM-EDS, abiotic oxidation. Biol. Fertil. Soils 50, 623-632.
475 Feng, X., 2002. A theorethical analysis of carbon isotope evolution of decomposing plant litters and soil
476 organic matter. Global Biogeochem. Cy. 16, 1119.
477 Fitzpatrick, E.A., 1980. Soils: their formation, classification and distribution. London, Longman.
478 FitzPatrick E.A., 1993. Soil microscopy and micromorphology. J Wiley & Sons, Chichester.
479 Gee, G., Bauder, J.W., 1986. Particle-size analysis, in: Klute, A. (Ed.), Methods of soil analysis: Part1, 2nd ed.
480 Agron. Monogr. No. 9 ASA and SSSA, Madison, WI, pp. 383-411.
481 Geisseler, D., Horwath, W.R., Scow, K.M., 2011. Soil moisture and plant residue addition interact in their
482 effect on extracellular enzyme activity. Pedobiologia 54, 71-78.
483 Giacometti, G., Cavani, L., Baldoni, G., Ciavatta, C., Marzadori, C., Kandeler, E., 2014. Microplate-scale
484 fluorometric soil enzyme assays as tools to assess soil quality in a long-term agricultural field experiment.
485 Appl. Soil Ecol. 75, 80–85.

Gioacchini, P., Cattaneo, F., Barbanti, L., Montecchio, D., Ciavatta, C., Marzadori, C., 2016. Carbon sequestration and distribution in soil aggregate fractions under Miscanthus and giant reed in the Mediterranean area. Soil Till. Res. 163, 235-242.

Hallaire, v., Curmi, P., Duboisset, A., Lavelle, P., Pashanasi, B. 2000. Soil structure changes induced by the tropical earthworm *Pontoscolex corethrurus* and organic inputs in a Peruvian ultisol. Eur. J. Soil Biol. 36, 35−44.

Heckman, K., Lawrence, C.R., Harden, J.H., 2018. A sequential selective dissolution method to quantify storage and stability of organic carbon associated with Al and Fe hydroxide phases. Geoderma 312, 24-35.

Ismail-Meyer, K., Stolt, M.H., Lindbo, D.L., 2018. Chapter 17 - Soil Organic Matter. In: Stoops, G., Marcelino, V., Mees, F. (Eds). Interpretation of Micromorphological Features of Soils and Regoliths 2th Edition, Elsevier, pp. 471-512.

Kögel-Knabner, I., Guggenberg, G., Kleber, M., Kandeler, E., Kalbitz, K., Stefan, S., Eusterhues, K., Leinweber, P., 2008. Organo-mineral associations in temperate soils: integrating biology, mineralogy, and organic matter chemistry. J. Plant Nutr. Soil Sc. 171, 61-82.

Kravchenko, A.N., Guber, A.K., 2017. Soil pores and their contributions to soil carbon processes. Geoderma. 287, 31-39.

Kravchenko, A.N., Negassa, W.C., Guber, A.K., Rivers, M.L., 2015. Protection of soil carbon within macro-aggregates depends on intra-aggregate pore characteristics. Sci. Rep. 5, 16261-16261.

Janzen, H.H., 2004. Carbon cycling in earth systems-a soil science perspective. Agr. Ecosyst. Environ. 104, 399-417.

Lal, R., 2004a. Soil carbon sequestration impacts on global climate change and food security. Science 304, 1623-1626.

Lal, R., 2004b. Soil carbon sequestration to mitigate climate change. Geoderma 123, 1-22.

Lal, R., Negassa, W., Lorenz, K., 2015. Carbon sequestration in soil. J. Environ. Sustain. 15, 79-86.

Legout, C., Leguédoi, S., Le Bissonnais, Y., 2005. Aggregate breakdown dynamics under rainfall compared with aggregate stability measurements. Eur. J. Soil Sci. 56, 225-237.

512 Liu, Y. R., Li, X., Shen, Q. R., & Xu, Y. C., 2013. Enzyme activity in water-stable soil aggregates as affected by
513 long-term application of organic manure and chemical fertiliser. Pedosphere 23, 111–119.
514 Lu, J., Zheng, F., Li, G., Bian F., An, J., 2016. The effects of raindrop impact and runoff detachment on hillslope
515 soil erosion and soil aggregate loss in the Mollisol region of Northeast China. Soil Till. Res. 161, 79-85.
516 Mikutta, R., Kleber, M., Torn, M.S., Jahn R., 2006. Stabilization of soil organic matter association with minerals
517 or chemical recalcitrance? Biogeochemistry 77, 25-56.
518 Nakatsuka, H., Tamura, K., 2016. Characterisation of soils under long-term crop cultivation without
519 fertilisers: a case study in Japan. SpringerPlus 5, 283.
520 Pagliai, M., Vignozzi, N., Pellegrini, S., 2004.Soil structure and the effect of management practices. Soil Till.
521 Res. 79, 131-143.
522 Poeplau, C., Don, A., Six, J., Kaiser, M., Benbi, D., Chenu, C., Cotrufo, M.F., Derrien, D., Gioacchini, P., Grand,
523 S., Gregorich, E., Griepentrong, M., Gunina, A., Haddix, M., Kuzyakov, Y., Kuhnel, A., Macdonald, L.M., Soong,
524 J., Trigalet, S., Vermeirc, ML., Rovira, P., van Wesemael, B., Wiesmeier, M., Yeasmin, S., Yevdokimov, I.,
525 Nieder, R., 2018. Isolating organic carbon fraction with varying turnover rates in temperate agricultural soils
526 - A comprehensive method comparison. Soil Biol. Biochem. 125, 10-26.
527 Qin, S. P., Hu, C. H., He, X. H., Dong, W. X., Cui, J. F. Wang, Y. 2010. Soil organic carbon, nutrients and relevant
528 enzyme activities in particle-size fractions under conservational versus traditional agricultural management.
529 Appl. Soil Ecol. 45: 152–159.
530 Quigley, M.Y., Negassa, W.C., Guber, A.K., Rivers, M.L., Kravchenko, A.N. 2018. Influence of pore
531 characteristics on the fate and distribution of newly added carbon. Front. Environ. Sci. 6, 51.
532 R Core Team, 2019. R: A language and environment for statistical computing.
533 Schmidt, M.W.I., Torn, M.S., Abiven, S., Dittmar, T., Guggenberger, G., Janssen, I.A., Kleber, M., Knabner, I.K.,
534 Lehmann, J., Manning, D.A., Nannipieri, P., Rasse, D.P., Weiner, S., Trumbore, S.E., 2011. Persistance of soil
535 organic matter as an ecosystem property. Research Perspective 478, 49-56.
536 Regione Emilia Romagna, 2018. Carta dei suoli della pianura, del basso e medio appennino emiliano-
537 romagnolo in scala 1:50.000. Servizio Geologico, Sismico e dei Suoli della Regione Emilia Romagna.

538 Sarker, T.C., Incerti, G., Spaccini, R., Piccolo, A., Mazzoleni, S. Bonanomi, G., 2018. Linking organic matter
539 chemistry with soil aggregate stability: Insight from 13C NMR spectroscopy. Soil Biol. Biochem. 117, 175–184.
540 Six, J., Elliot, E.T., Paustian, K., 2000. Soil macroaggregate turnover and microaggragate formation: a
541 mechanism for C sequestration under no-tillage agriculture. Soil Biol. Biochem. 32, 2099-2103.
542 Six, J., et al., 2002. Soil organic matter, biota and aggregation in temperate and tropical soils effect of no
543 tillage. Agronomie 22, 755-775.
544 Six, J., Bossuyt, H., Degryze, S., Denef, K., 2004. A history of research on the link between (micro)aggregates,
545 soil biota, and soil organic matter dynamics. Soil Till. Res. 79, 7–31.
546 Smith, P., Fang C., Dawson, J.J.C., Moncrieff. J.B., 2008. Impact of global warming on soil organic carbon. Adv.
547 Agron. 97, 1-43.
548 Soil Survey Staff. 2014. Keys to Soil Taxonomy, 12th ed. USDA-Natural Resources Conservation Service,
549 Washington, DC.
550 Stoops G., 2003. Guidelines for Analysis and Description of Soil Regolith Thin-Sections. Soil Science Society of
551 America, Madison.
552 Takeda, H. 1988. A rapid method for preparing thin sections of soil organic layers. Geoderma 42, 159-164
553 Tippkötter, R., Ritz, K., Darbyshire, J.F., 1986. The preparation of soil thin sections fo biological studies. Eur.
554 J. Soil Sci. 37, 681-690.
555 Tisdall J.M., Oades J.M.. 1982. Organic matter and water-stable aggregates in soils. J. Soil Sci. 33:141–163.
556 Totsche, K.U., Martin, W.A., Gerzabek H., Guggenberger G., Klumpp E., Knief C., Lehndorff E., Mikutta R.,
557 Peth S., Prechtel A., Ray N., Kögel-Knabner, I., 2017, Microaggregates in soils. J. Soil Sci. Plant Nutr. 181, 104-
558 163.
559 Toosi, E. R., Kravchenko, A. N., Mao, J., Quigley, M. Y., and Rivers, M. L., 2017. Effects of management and
560 pore characteristics on organic matter composition of macroaggregates: evidence from characterization of
561 organic matter and imaging. Eur. J. Soil Sci. 68, 200-211.
562 Van Reeuwijk, L.P., 2002.Procedures for soil analysis. Technical Paper n. 9. International Soil Reference and
563 Information Centre, Wageningen, 11-1.

564 Vittori Antisari, L., Carbone, S., Gatti, A., Vianello, G., Nannipieri, P., 2014. Uptake and translocation of metals
565 and nutrients in tomato grown in soil polluted with metal oxide ($CeO_2$, $Fe_3O_4$, $SnO_2$, $TiO_2$) or metallic (Ag, Co,
566 Ni) engineered nanoparticles. Environ. Sci. Pollut. Res. 22, 1841-1853.
567 Wang, Y. Hu, N., Ge, T., Kuzyakov, Y., Wang, Z-L., Li, Z., Tang, Z., Chen, Y., Wu, C., Lou, Y. 2017. Soil aggregation
568 regulates distributions of carbon, microbial community and enzyme activities after 23-year manure
569 amendment. Appl. Soil Ecol. 111, 65-72
570 Wang, R., Dorodnikov, M., Yang, S., Zhang, S., Zhang, Y., Filley, T.R., Turco, R.F., Zhang, Y., Xu, Z., Li, H., Jiang,
571 Y. 2015. Responses of enzymatic activities within soil aggregates to 9-year nitrogen and water addition in a
572 semi-arid grassland. Soil Biol. Biochem. 81, 159-167.
573 Wiesmeier, M., Urbanski, L., Hobley, E., Lang, B., von Lutzow, M., Marin-Spiotta, E., van Wesemael, B., Rabot,
574 E., LieB, M., Gracia-Franco, N., Wollschager, U., Vogel, HJ., Kögel-Knabner, I., 2019. Soil organic carbon
575 storage as a key function of soil – A rewiew of drivers and indicatori at various scales. Geoderma 333, 149-
576 162.
577 Yang, C., Liu, N., Zhang, Y., 2019, Soil aggregates regulate the impact of soil bacterial and fungal communities
578 on soil respiration. Geoderma 337, 444-452.
579 Young I.M., Crawford J.W., Nunan N., Otten W., Spiers A., 2008. Microbial distribution in soils: physics and
580 scaling, in: Sparks, D.L. (Ed.). Advances in Agronomy. Academic Press, Burlington, pp. 81–121.
581 Zhou, H., Peng, X., Pech, S., Xiao, T.Q., 2012. Effects of vegetation restoration on soil aggregates
582 microstructure quantified with synchrotron-based micro-computed tomography. Soil Till. Res. 124, 17-23.
583

584

585 **Figure captions**

586 Figure 1. Pore size distribution in a) coarse and b) fine macroaggregates. In c) the ANOVA results are
587 reported. M-OW and M-AA: 16-yrs old oak wood and 5-yrs old alfalfa in mountain area, respectively; P-NF
588 and P-FF: non-fertilized and fertilized walnut grove in plain area.

589 Figure 2. Al:C, Fe:C and Ca:C molar ratio of the different organic forms in coarse and fine macroaggregates.
590 Different capital letters represent the significant diffences among organic forms. Different lower letters
591 represent the significant difference between coarse and fine macroaggregates within the same organic
592 forms.

593 Figure 3. Box-plots of exposure index (EI, in $mm^{-1}$) values in the coarse and fine macroaggregates. The box
594 represents the interquartile range, the line represents the median value, the symbol represents the mean
595 value, error bars represent the full range of data. Different letters refer to significant differences ($p<0.05$)

596 Figure 4. Relationships between EI values measured in aggregate thin sections and chemical properties
597 measured on ground aggregates (C/N ratio and $\delta^{13}C$). The coarse (filled symbols) and fine macroaggregate
598 (open symbols) classes are display for each plot. The error bars indicate the standard deviation.

599 Figure 5. Relationships between EI values measured in aggregate thin sections and geometric mean of
600 assayed enzyme activities (GM*ea*). The coarse (filled symbols) and fine macroaggregate (open symbols)
601 classes are display for each plot. The error bars indicate the standard deviation.

602 Figure 6. Conceptual scheme of macroaggregates and organic matter stabilization. Into brackets the
603 microfeatures used in this study and suggesting each step of the scheme

604

Figure 1

Click here to access/download;Figure;Figure 1.pptx

a)

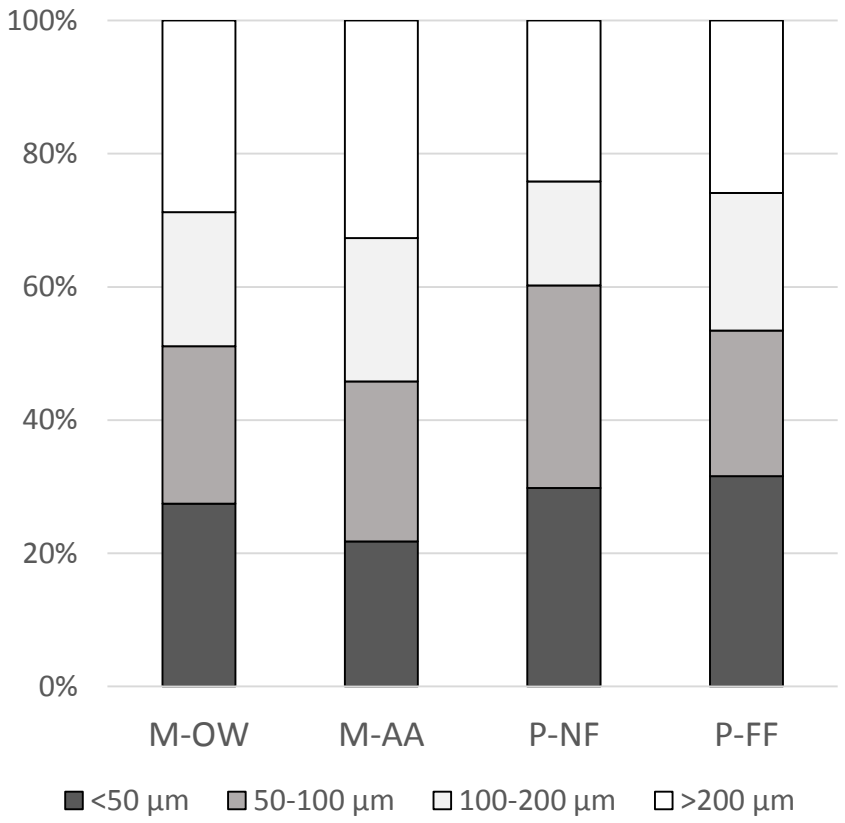


b)

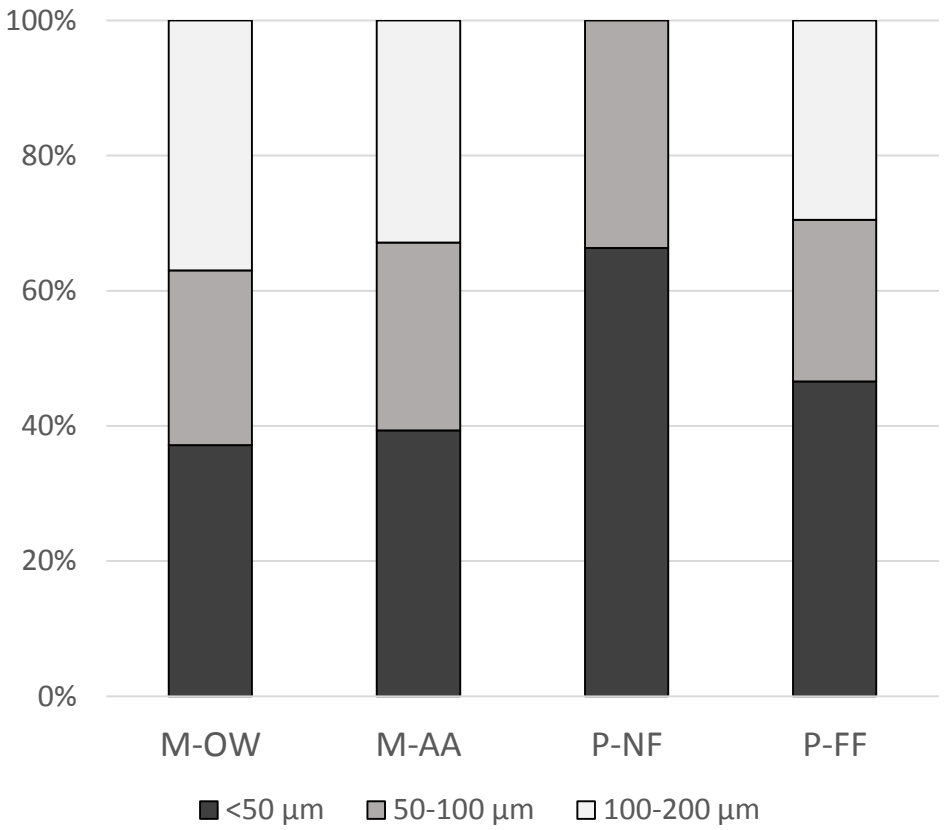


c)

| | | <50 µm (%) | 50-100 µm (%) | 100-200 µm (%) | >200 µm (%) |
|---|---|---|---|---|---|
| coarse *vs* fine macroaggregates | | *** | ** | *** | nd |
| within coarse macroaggregates | site | ns | ns | ns | ns |
| within fine macroaggregates | site | ns | ns | ns | nd |

ns: not significant (p>0.05);*: p<0.05; **: p<0.01; ***: p<0.001

nd: not determined

Figure 2



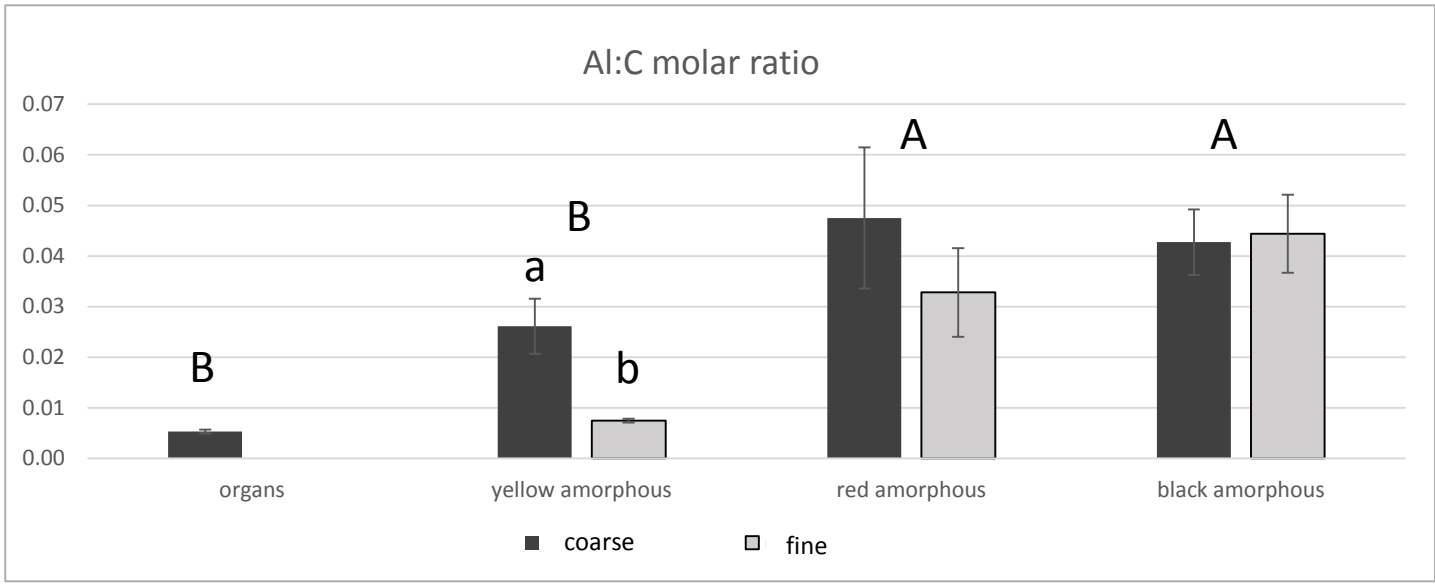


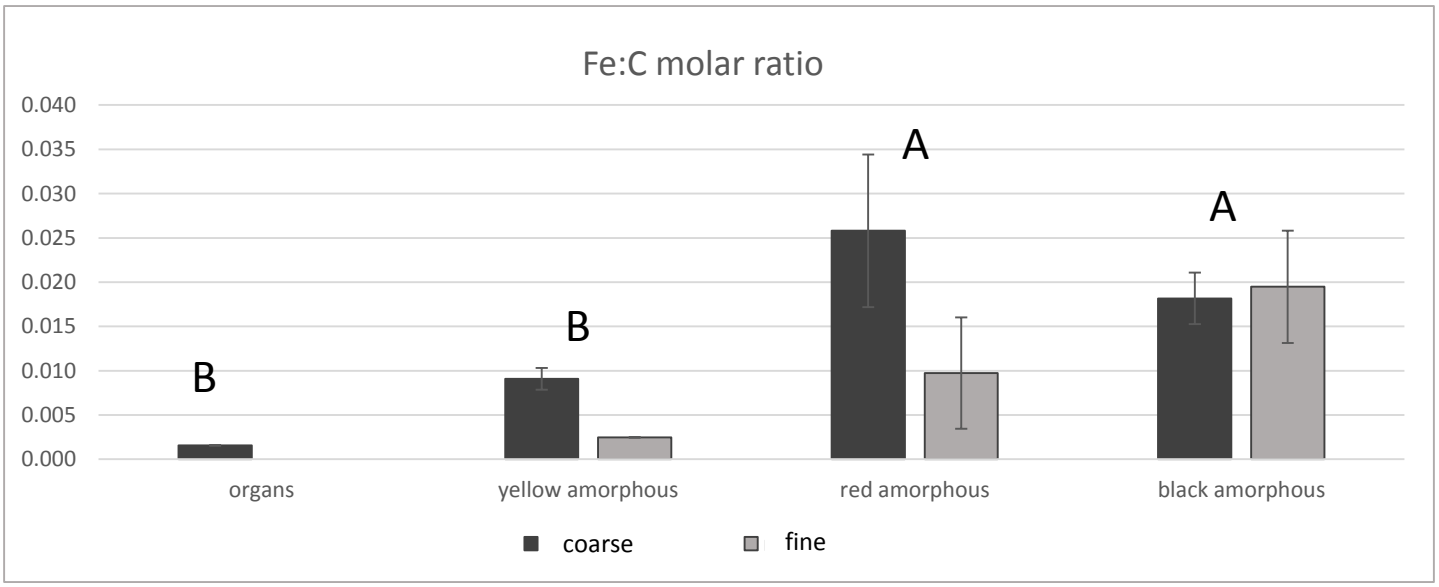


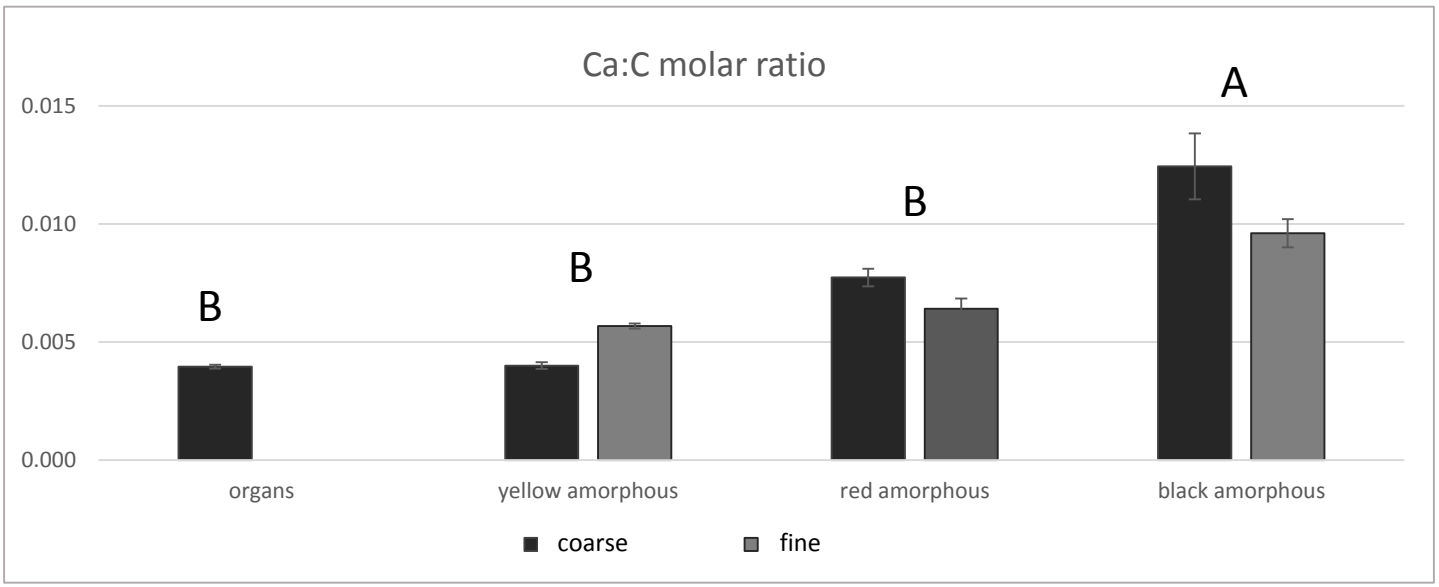

Figure 3



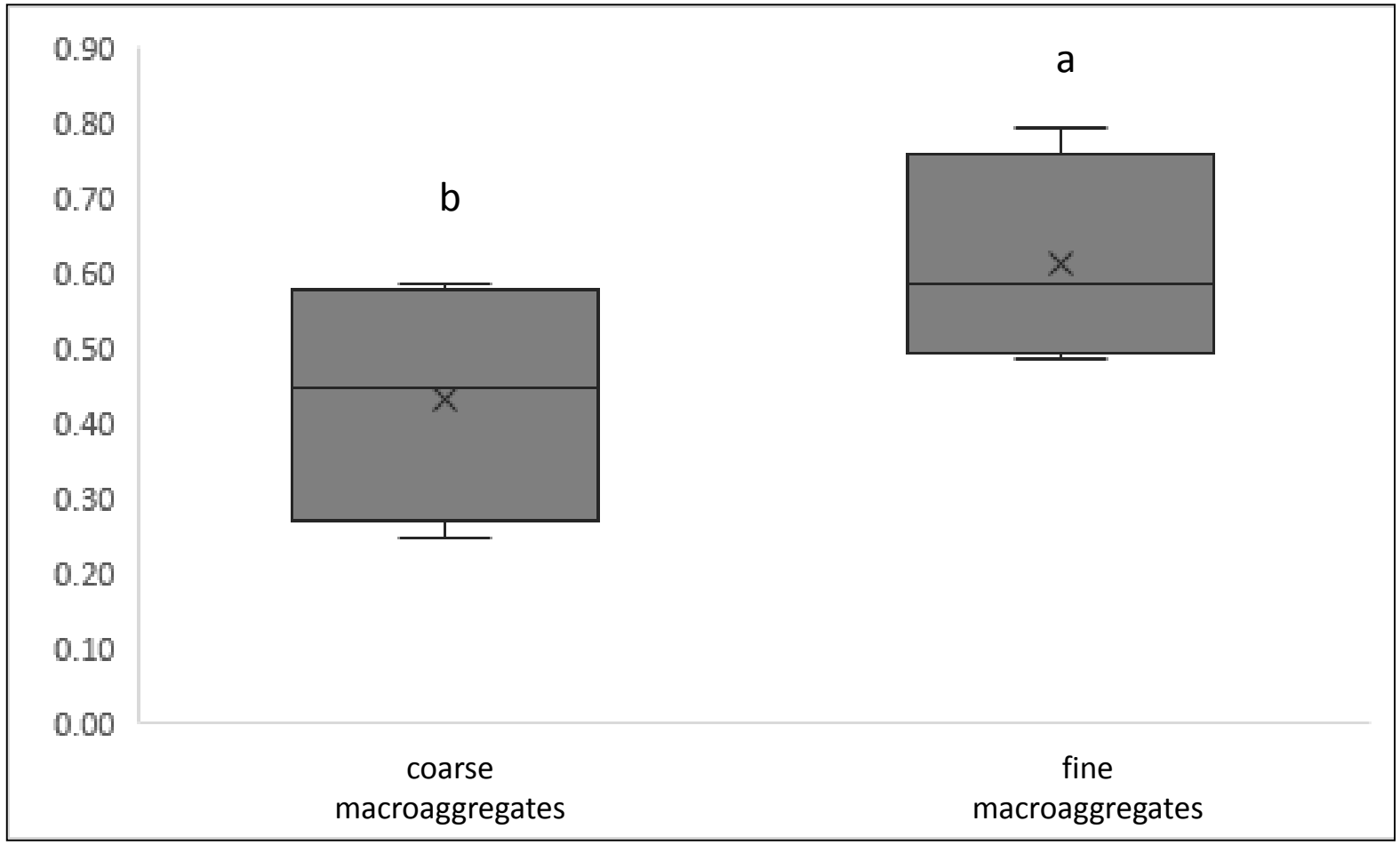

Figure 4



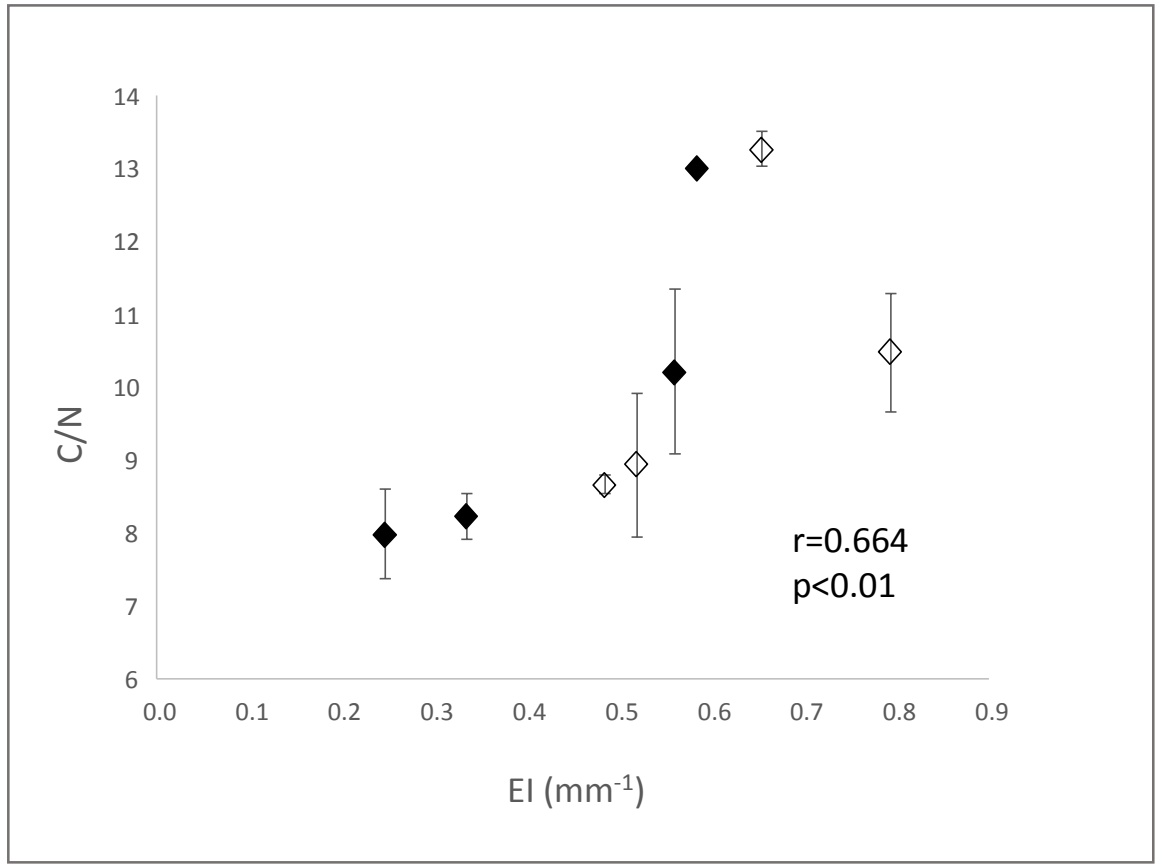


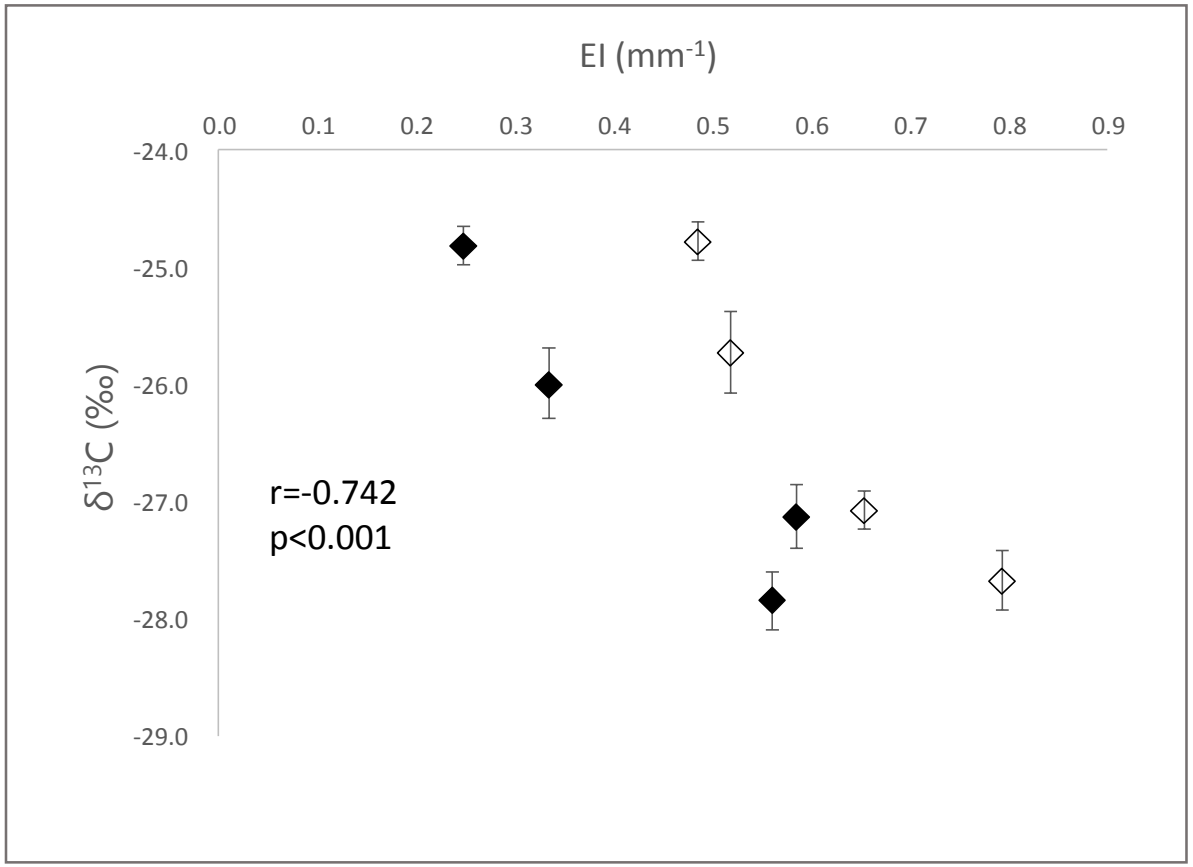

Figure 5

Click here to access/download;Figure;Figure 5.pptx

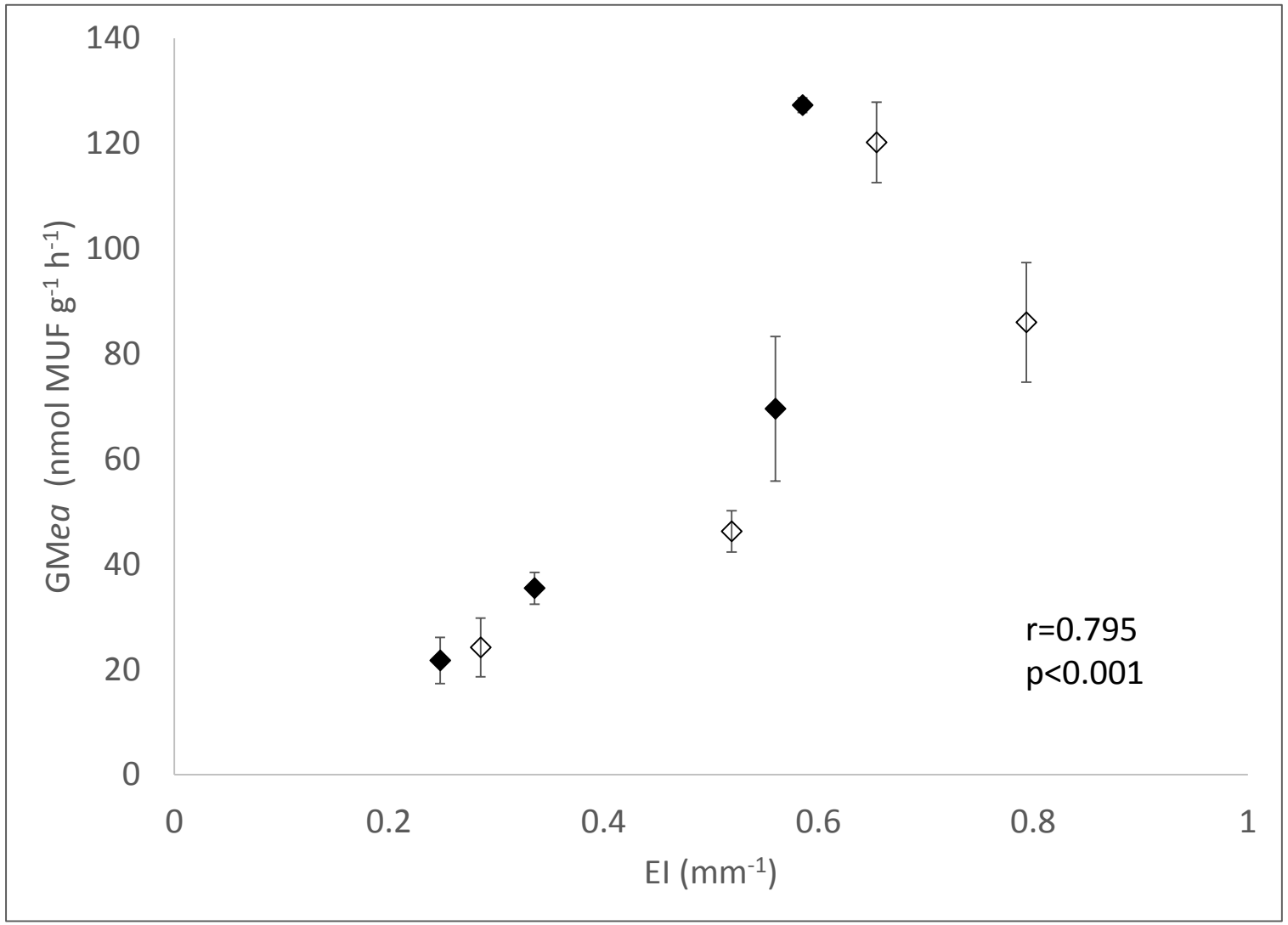

Figure 6



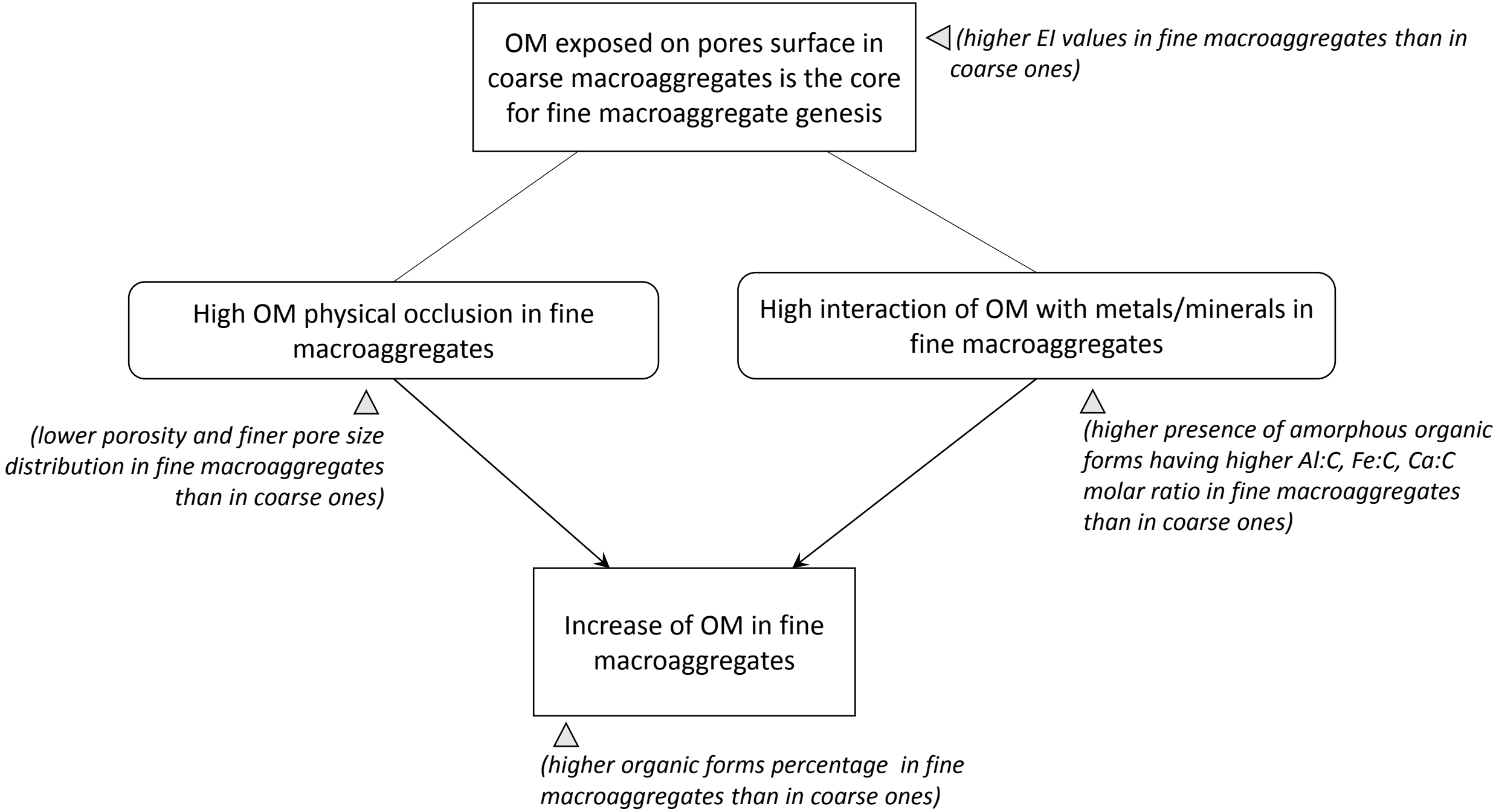

Table 1. General information of the investigated sites

| Area (climate/soil type) | Site | Coordinates | Elevation (m a.s.l.) | Soil management and sampling information |
|---|---|---|---|---|
| Mountain (MAT: 11.6°C; MAP: 967 mm/Inceptisols) | M-OW | 44° 16’29’’N 11°14’53’’E | 630 | The oak wood was a 16-year-old wood exploited for firewood. At sampling time, the wood was at the end of its cutting cycle. |
| | M-AA | 44°16’28’’N 11°15’25’’E | 663 | The alfalfa was a 5-year-old crop not-fertilizer. At sampling time, the alfalfa was at the end of its cropping cycle. |
| Plain (MAT: 12.9°C ; MAP: 645 mm/Inceptisols) | P-FF | 44°32’18’’N 11°23’07’’E | 34 | Since 2001, 90 kg/ha/yr g of urea has been distributed for granular treatment subdividing in two doses (45 kg/ha/yr g in April/May and 45 kg/ha/yr in October). The soil was not tilled and covered by spontaneous grasses. The soil sampling was done along the plant rows. |
| | P-NF | 44°32’19’’N 11°23’07’’E | 34 | Since 2001, the site was not fertilized. The soil was not tilled and covered by spontaneous grasses. The soil sampling was done along the plant rows. |

MAT: mean annual temperature; MAP: mean annual precipitation

Table 2. Percentage of total porosity, organic carbon and presence of organic matter forms in coarse and fine macroaggregates. Numbers in the brackets represent the standard deviation values. In the bottom, the ANOVA results are reported

| Macroaggregate class | Sites | Total porosity[a] (%) | Organic carbon[b] g $kg^{-1}_{aggregate}$ | Organic matter forms[a] (%) |
|---|---|---|---|---|
| coarse | M-OW | 5.96 (1.67) | 49.6 (4.6) | 8.27 (1.29) |
| | M-AA | 9.08 (1.00) | 10.9 (3.5) | 6.51 (0.95) |
| | P-NF | 5.93 (1.89) | 6.6 (1.8) | 4.19 (0.88) |
| | P-FF | 8.19 (1.43) | 7.9 (1.2) | 5.58 (1.10) |
| fine | M-OW | 4.42 (0.97) | 52.4 (7.3) | 17.2 (4.48) |
| | M-AA | 6.71 (1.43) | 12.1 (3.4) | 17.7 (1.94) |
| | P-NF | 3.70 (0.78) | 7.8 (1.2) | 14.4 (2.99) |
| | P-FF | 6.53 (1.18) | 9.3 (3.0) | 13.5 (3.41) |
| coarse *vs* fine macroaggregates | | *** | ns | *** |
| within coarse macroaggregates | site | ns | *** | ns |
| within fine macroaggregates | site | ns | ** | ns |

[a]measured on macroaggregate thin sections; [b]measured on grounded macroaggregates.

M-OW and M-AA: 16-yrs old oak wood and 5-yrs old alfalfa in mountain area, respectively; P-NF and P-FF: non-fertilized and fertilized walnut grove in plain area.

ns: not significant ($p>0.05$); **:$p<0.01$; ***: $p<0.001$

Table 3. Organic matter forms distribution in coarse and fine macroaggregates. Numbers in the brackets represent the standard deviation values

| macroaggregate class | sites | Organs (%) | Yellow amorphous forms (%) | Red amorphous forms (%) | Black amorphous forms (%) |
|---|---|---|---|---|---|
| coarse | M-OW | 3.31 (0.9) | 1.87 (0.2) | 2.32 (0.6) | 3.16 (0.7) |
| | M-AA | 1.11 (0.4) | - | 2.09 (0.9) | 3.51 (0.3) |
| | P-NF | - | 1.10 (0.4) | 1.29 (0.3) | 2.07 (0.4) |
| | P-FF | - | 1.10 (0.5) | 2.14 (0.5) | 3.14 (0.7) |
| fine | M-OW | - | 1.21 (0.4) | 7.77 (0.8) | 8.51 (1.2) |
| | M-AA | - | 1.84 (0.8) | 6.07 (0.7) | 12.1 (1.2) |
| | P-NF | - | - | 6.64 (0.7) | 9.72 (1.5) |
| | P-FF | - | - | 5.65 (0.8) | 5.30 (0.9) |
| coarse *vs* fine macroaggregates | | - | - | *** | *** |
| within coarse macroaggregates | site | - | - | * | * |
| within fine macroaggregates | site | - | - | *** | *** |

M-OW and M-AA: 16-yrs old oak wood and 5-yrs old alfalfa in mountain area, respectively; P-NF and P-FF: non-fertilized and fertilized walnut grove in plain area.

ns: not significant ($p>0.05$); *:$p<0.05$; ***: $p<0.001$

**Declaration of interests**

☒ The authors declare that they have no known competing financial interests or personal relationships that could have appeared to influence the work reported in this paper.

☐The authors declare the following financial interests/personal relationships which may be considered as potential competing interests: